Absence of an Ideal Single-Walled Carbon Nanotube Forest Structure for Thermal and Electrical Conductivities

Guohai Chen,[†,‡] Don N. Futaba,[†,‡,*] Hiroe Kimura,[†,‡] Shunsuke Sakurai,[†,‡] Motoo Yumura,[†,‡] and Kenji Hata[†,‡,§,*]

[†]Technology Research Association for Single Wall Carbon Nanotubes (TASC), Central 5, 1-1-1 Higashi, Tsukuba, Ibaraki 305-8565, Japan, [‡]National Institute of Advanced Industrial Science and Technology (AIST), Central 5, 1-1-1 Higashi, Tsukuba, Ibaraki 305-8565, Japan, and [§]Japan Science and Technology Agency (JST), Honcho 4-1-8, Kawaguchi 332-0012, Japan

ABSTRACT We report the fundamental dependence of thermal diffusivity and electrical conductance on the diameter and defect level for vertically aligned single-walled carbon nanotube (SWCNT) forests. By synthesizing a series of SWCNT forests with continuous control of the diameter and defect level over a wide range while holding all other structures fixed, we found an inverse and mutually exclusive relationship between the thermal diffusivity and the electrical conductance. This relationship was explained by the differences in the fundamental mechanisms governing each property and the optimum required structures. We concluded that high thermal diffusivity and electrical conductance would be extremely difficult to simultaneously achieve by a single SWCNT forest structure within current chemical vapor deposition synthetic technology, and the "ideal" SWCNT forest structure would differ depending on application.

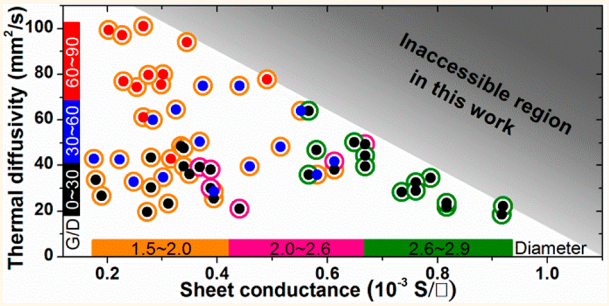

KEYWORDS: single-walled carbon nanotube · SWCNT forest · diameter · crystallinity · thermal diffusivity · electrical conductance

Nanomaterials, as represented by carbon nanotubes (CNTs), are a peculiar class of materials different from conventional chemical substances. Unlike conventional chemical materials where the structure is uniquely defined by a structural formula, an infinite number of structures fall under the name, CNTs. For example, CNTs differ in structure by the chirality, diameter, wall number, length, defect level (crystallinity), defect type, straightness, *etc.* This structural diversity is one of the central issues of CNT research and its use for practical applications since the physical and chemical properties of a CNT are known to critically depend on its structure.[1−4] For example, only a small difference in chirality in a single-walled CNT (SWCNT) separates semiconducting and metallic electronic behavior highlighting the significant impact of the structure on the properties.[4]

Structural control of CNTs has been pursued by numerous researchers, and now the CNT field has developed synthetic structural control in diverse directions as exemplified by control of chirality, alignment/density, diameter, wall number, defect density, and semiconducting-metallic selective growth.[5−15] For instance, a selective growth of over 95% semiconducting SWCNT has been reported by using methanol.[5] Aligned CNT forests with ultrahigh density of $\sim 10^{13}$ cm^{-2} have been achieved through cyclic catalyst deposition.[6] Control of the SWCNT diameter has been demonstrated from 1.3 to 2.1 nm by the floating catalyst method.[7] SWCNTs with a single dominating chirality, (8,4), have been synthesized by using a $Ni_{0.27}Fe_{0.73}$ nanocatalyst.[8]

Although the structural control of various aspects of the CNTs have been previously reported in the literature, research investigating the dependence of structure on the physical properties (such as electrical and thermal) has not yet reached the level where the fundamental relationship between a physical property and a structure is clearly empirically known.[1,2,16−21] Previously, most

* Address correspondence to kenji-hata@aist.go.jp, d-futaba@aist.go.jp.

Received for review August 29, 2013 and accepted October 3, 2013.

Published online October 03, 2013
10.1021/nn404504f

such reports have been limited to comparisons between different CNTs (*e.g.*, HiPco, CoMoCAT, Nanocyl, *etc*. where all of the CNT structures are different) often made from different suppliers, which were then processed into a particular form, such as transparent conductive film (TCF), buckypaper, fiber, composite, *etc*.[18−21] For example, a comparative study has shown that TCFs using arc discharge SWCNTs exhibited a 1 order of magnitude higher sheet conductance than that using HiPco SWCNTs at similar optical transparencies.[18] In addition, a comparison of SWCNT/polystyrene composites between HiPco, CoMoCAT, and pulsed laser vaporization CNTs has shown that composites made with HiPco tubes exhibited the highest electrical conductivity (about 2 orders of magnitude higher) at >1 wt % CNT loading.[19] Another comparison of CNT/elastomer composites, using CoMoCAT, HiPco, and water-assisted chemical vapor deposition (CVD) SWCNTs (SG-SWCNTs), and Nanocyl multiwalled CNTs (MWCNTs) has shown that only the SG-SWCNT composite showed high electrical conductivity with excellent mechanical durability.[20] By this comparative research, one can only conclude which variety CNT was optimum for a specific application, but one cannot determine the intrinsic properties of CNTs and their dependence on structure for the purpose of a more general understanding of the most suitable CNT structure for a given application.

In this work, we have addressed this issue and studied the fundamental dependence of thermal diffusivity and electrical conductance on the diameter and defect level for vertically aligned SWCNT forests. Such investigation was enabled by synthesizing a series of SWCNT forests with diverse and controlled structures spanning a wide range of average diameters (1.5−2.9 nm) and defect levels (as represented by Raman graphitic-to-disorder ratio, *e.g.*, G/D ratio: ∼2 to ∼90). Significantly, we found a mutual exclusivity between the thermal diffusivity and the electrical conductance, where small average diameter SWCNT forests exhibited the highest thermal diffusivities while large average diameter SWCNT forests provided the highest electrical conductances. We interpret that such mutual exclusivity stems from a combination of several fundamental mechanisms, such as the reduced Umklapp scattering in smaller diameter SWCNT forests, which allows for higher thermal diffusivity, and the reduced band gap for larger diameter SWCNT forests, which leads to higher electrical conductance. These results and interpretations demonstrate that the highest thermal diffusivity and electrical conductance cannot be simultaneously achievable on the same SWCNT forest structure within current CVD synthetic technology where both semiconducting and metallic SWCNTs co-exist, and the "ideal" SWCNT forest structure would differ depending on application.

RESULTS AND DISCUSSION

To study the dependence of the properties on structures, several fundamental requirements are required. One must first identify all the structures that contribute to the property. Second, one must be able to control one or two of these structures while holding all the others fixed. Third, to construct a plot of the property as a function of structure, the synthetic control must be continuous rather than scattered. These fundamental requirements have been the obstacle in experimentally relating the properties to structures.

To satisfy these requirements, we synthesized a series of vertically aligned SWCNT forests with heights of ∼300 μm, differing by a wide range and in a continuous fashion in both diameter and defect level (crystallinity), by water-assisted CVD.[22] We used a well-established method of tailoring the Fe film thickness to control the average diameter of the SWCNT forest. In most previous works, this technique was used to control the average diameter and the wall number of CNTs. Here, we combined this technique with a trilayer catalyst (Al_2O_3/Fe/Al) technique developed by Kawarada/Roberson.[23,24] The alumina capping layer and the lower alumina support suppressed Fe surface diffusion and subsurface diffusion into the substrate, respectively, to allow the formation of small catalyst nanoparticles. Through this combination, we could significantly control the diameter range from 1.5 to 2.9 nm with a resolution of ∼0.1 nm.

Specifically, we divided the CVD process into three phases: a catalyst deposition phase (*i.e.*, a sputter phase in this work), a nanoparticle catalyst formation phase, and a growth phase (Figure 1a). The key process in this work was the "formation" phase where the deposited catalyst thin film was reduced in hydrogen ambient at high temperature to form nanoparticles. In fact, exposure of Fe catalyst thin film to hydrogen ambient at high temperature prior to the growth phase is the standard process to form catalyst nanoparticles needed for CNT synthesis. In this work, we decoupled the formation phase from the CNT growth phase to form catalyst nanoparticles at different temperature from 550 to 750 °C while keeping the growth temperatures fixed at 750 °C. Since the catalyst formation phase and growth phase were separated and the use of the alumina cap and alumina support provided considerable control on the individual catalyst particles, a series of ∼370 SWCNT forests could be synthesized where the diameter and defect level (G/D ratio) were continuously controlled across a wide range (average diameter, 1.5−2.9 nm; G/D ratio, ∼2 to ∼90) while holding the mass density and height fixed (height, ∼300 μm; mass density, ∼0.03 g/cm^3, within ∼20%). We would like to note that the diameter and defect level are two key structural parameters that influence the physical properties, such as electrical and thermal

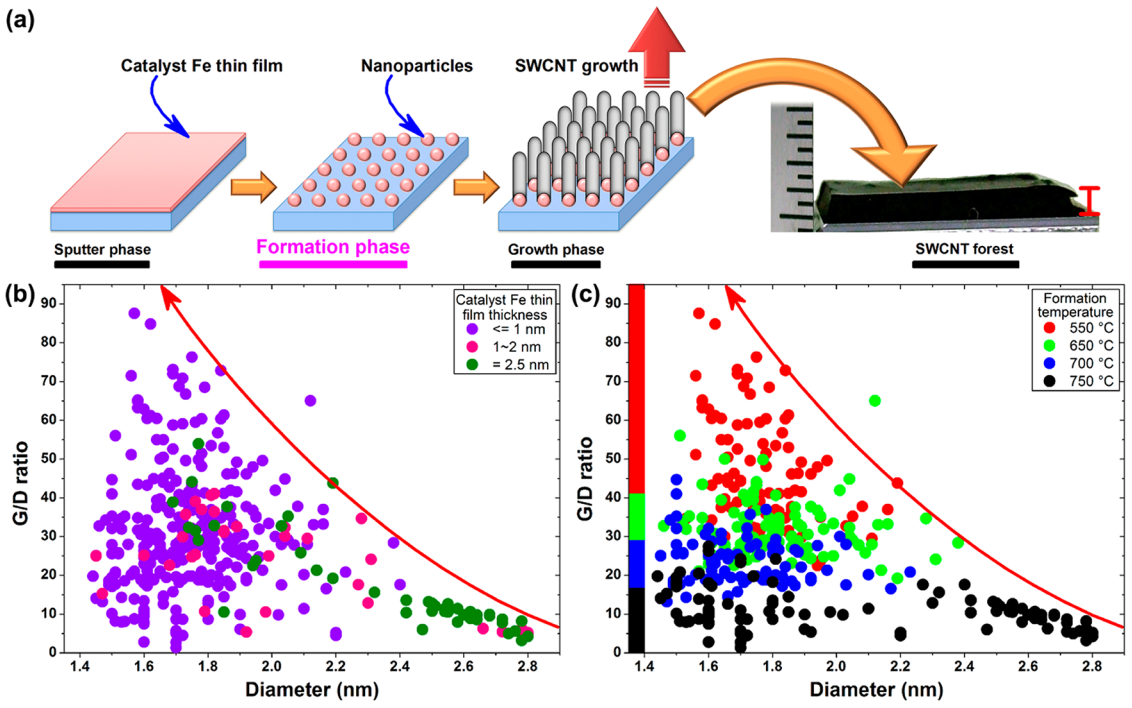

Figure 1. (a) Schematic of synthesizing SWCNT forests by tailoring Fe thin film thickness and formation temperature. G/D ratio of SWCNT forests as a function of diameter grouped by (b) catalyst Fe thin film thickness and (c) formation temperature. The red arrows are to guide the eyes.

conductivities of CNTs. Such a family of SWCNT forests synthesized by this advanced CVD technique satisfies the fundamental requirements presented above and provides a unique opportunity to investigate the dependence of the diameter and defect level on the electrical and thermal properties of SWCNT forests.

This large ensemble of SWCNT forests enabled the investigation of the structural and physical properties. From the plot of the G/D ratio as a function of the diameter, we observed several points (Figure 1b). First, a clear inverse relationship appeared where smaller diameter exhibited higher G/D ratio. Second, a prominent vacant region within this plot was observable which showed a synthetically forbidden region for our samples. This indicates the difficulty in synthesizing high quality SWCNTs with large diameter at the same growth conditions as for SWCNTs. Third, catalyst Fe film thickness was a control parameter of diameter where, as indicated by color, thinner Fe thickness resulted in smaller diameter SWCNTs. This general trend can be clearly seen in the plot of CNT diameter *versus* catalyst Fe film thickness (Supplementary Figure S1). Furthermore, the data points, color coded by the catalyst formation temperature, indicate the increasing diameter with increasing formation temperature. Forth, it is interesting to note that despite being grown from the same Fe thickness, the defect level could greatly vary. For example, for 1 nm Fe catalyst thickness, the G/D ratio spanned from ~10 to ~90. To address this issue, we plotted the G/D ratios as a function of the diameter with data points grouped by catalyst formation temperature (Figure 1c). From this plot, we note that the nanoparticle formation temperature was a significant control parameter of the defect level where a lower formation temperature led to a lower defect level. Specifically, a formation temperature of 550 °C resulted in a G/D ratio from ~30 to ~90, but a formation temperature of 750 °C led to a G/D ratio from ~2 to ~25. These results imply that a smaller diameter SWCNT grown from catalyst nanoparticles formed at lower temperature was the key to achieve higher quality SWCNTs. Although the mechanism is not fully understood, it could be that the catalyst structures at high (fcc, γ-Fe, austenite) and low (bcc, α-Fe, ferrite) temperatures differ.[25]

We start from describing the dependence of the thermal diffusivity on the diameter and defect level. Thermal diffusivity is one of the most fundamental properties of CNTs and here was measured by the flash method using a Xenon lamp source at room temperature along the CNT growth (alignment) direction for the series of SWCNT forests and plotted *versus* the diameter and G/D ratio (Figure 2).[26] We can glean several important points from the plotted data. First, the thermal diffusivity increased as the diameter decreased. The overall thermal diffusivity data showed an increase from ~20 to ~100 mm^2/s. The highest value was close to that of copper (111 mm^2/s) and superior to aluminum (84.2 mm^2/s) and silicon (88 mm^2/s). Second, Figure 2a shows that the thermal diffusivity of small diameter SWCNT forests varied significantly demonstrating that the diameter was not the only

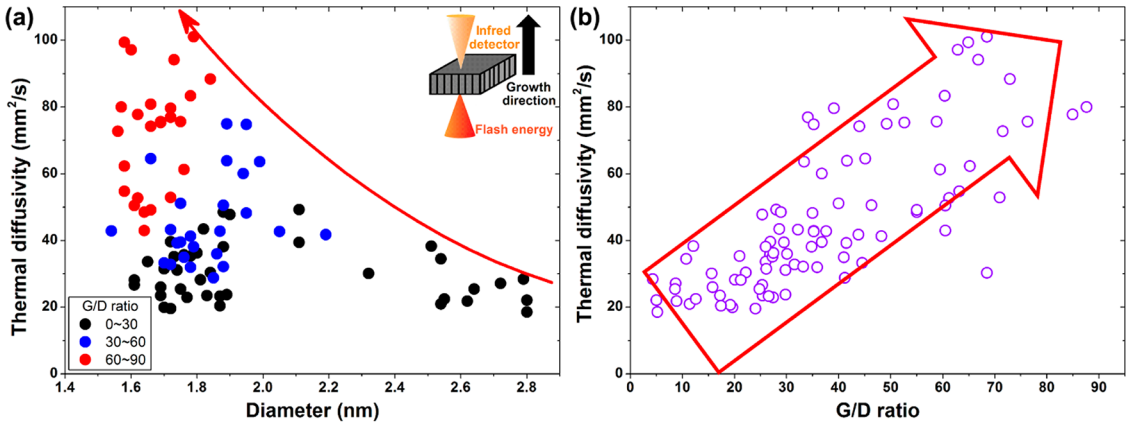

Figure 2. Thermal diffusivity of SWCNT forests as a function of (a) diameter and (b) G/D ratio. The red arrows are to guide the eyes. Inset: schematic of the measurement setup.

important parameter determining the thermal diffusivity. When we plotted the thermal diffusivity as a function of G/D ratio (Figure 2b), we found a nearly linear increase in thermal diffusivity from ~20 to ~100 mm^2/s as the G/D ratio rose from below 10 up to ~90, which experimentally demonstrated the direct effect of the defect level on the thermal diffusivity. These experimental data clearly demonstrated that smaller diameter SWCNT forests with higher crystallinity led to higher thermal diffusivity.

At room temperature for CNTs, it is known that phonon transport is the dominant contribution to the thermal diffusivity.[17,27,28] Phonon transport is disturbed by scattering by other phonons (Umklapp scattering) and crystalline defects. In short, Umklapp scattering is phonon−phonon scattering, which creates another phonon without conserving phonon momentum. Studies have shown that Umklapp scattering is reduced for smaller diameter SWCNTs because of the stronger phonon coupling from stronger curvature effects.[29−31] Simulations on diamond-like carbon, graphene and CNTs have reported that the thermal conductivity significantly drops with the presence of even a small level of defects.[32−35] This aspect has also been observed experimentally, where the thermal diffusivity of a vertically aligned MWCNT array increased from 42 to 210 mm^2/s due to the decrease in crystalline defects through a thermal annealing process (as evidenced by the increased Raman G/D ratio).[36]

From this discussion, we can gain deeper insight into the major scattering processes limiting the thermal diffusivity for our SWCNT forests. We interpret the data and propose that there are three domains that are governed by differing limiting processes. In the region of small diameter and high G/D ratio (specifically, diameter, 1.5−2.0 nm; G/D ratio, 60−90), the primary scattering process limiting the thermal diffusivity is Umklapp scattering. In the region of small diameter and low G/D ratio (diameter, 1.5−2.0 nm; G/D ratio, 2−30), the primary scattering process limiting the thermal diffusivity is defect scattering. In the third region of large diameter and low G/D ratio (diameter >2.4 nm and G/D ratio <15), we interpret that both Umklapp and defect scattering are significantly contributing.

Next, we describe the dependence of electrical sheet conductance on the diameter and defect level where, interestingly, we observed a strong but completely different dependence on the structures. The electrical sheet conductance here is the inverse of the electrical sheet resistance of SWCNT forests, which was measured along the CNT alignment direction with a home-made micro-4-probe (Figure 3, insets). The measured electrical sheet conductance of SWCNT forests was plotted *versus* the diameter and G/D ratio (Figure 3). As clearly shown, the electrical conductance strongly depended on the CNT structures but in a different manner than thermal diffusivity. In a complete reversal to the thermal diffusivity, the electrical conductance generally increased ~5-fold (from 0.2×10^{-3} to ~1.1×10^{-3} S/□) as the diameter increased (Figure 3a). It should be noted that the calculated CNT number density in the forests was found to be fairly constant across the diameter range (Supplementary Figure S2). Therefore, we do not attribute the number density as a significant factor in the electrical measurements. At this moment within this measurement technique, the conversion from sheet conductance to conductance per tube is not possible because the number of CNTs contributing to this measurement (*i.e.*, the depth) is unknown. There may be deviation originating either from the limitation of the measurement to a bulk sample rather than an individual CNT and/or from the internal structure of the forest, such as a broad diameter distribution, alignment, number of inter-tube contacts, *etc.* When we plotted the electrical conductance as a function of G/D ratio (Figure 3b), the electrical conductance surprisingly did not show any obvious dependence on the defect level and was fairly constant, which completely differed from the thermal diffusivity.

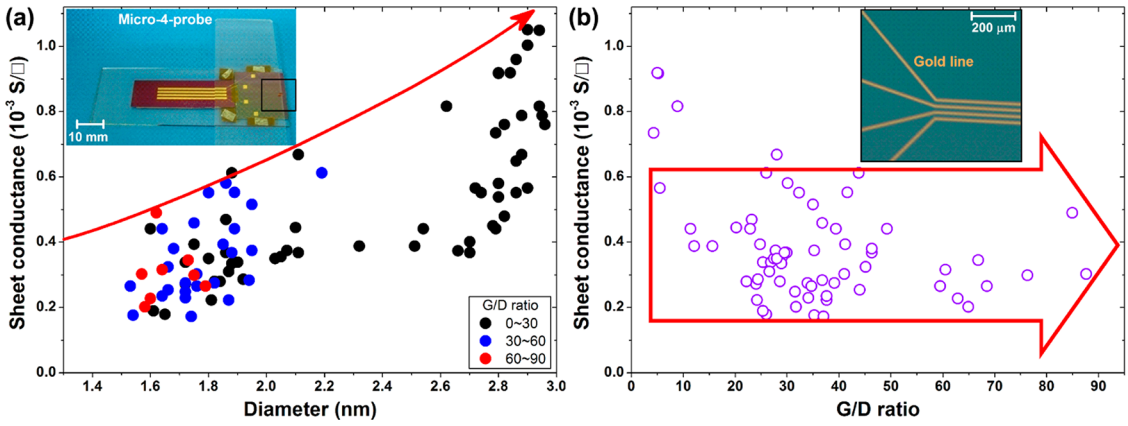

Figure 3. Electrical sheet conductance of SWCNT forests as a function of (a) diameter and (b) G/D ratio. The red arrows are to guide the eyes. Inset: (a) photo of the micro-4-probe; (b) magnified measurement area.

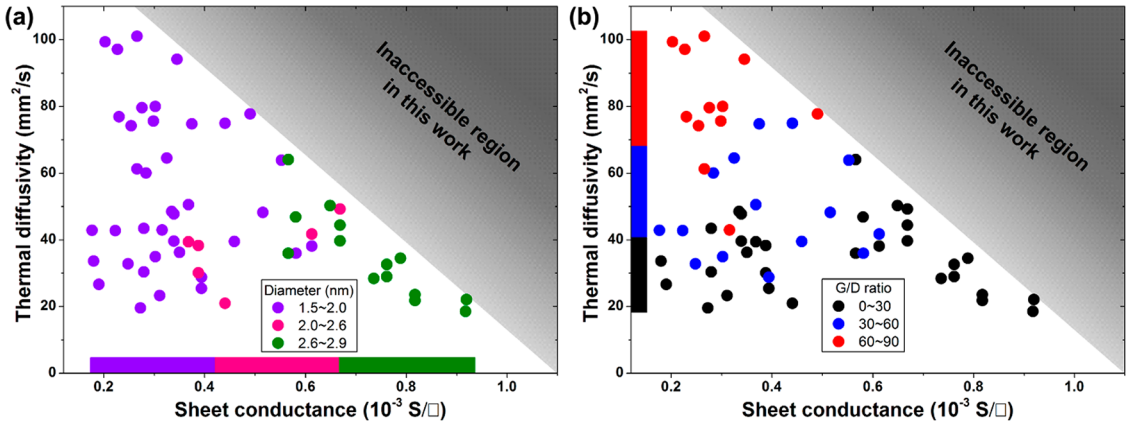

Figure 4. Thermal diffusivity *versus* electrical sheet conductance of SWCNT forests grouped by (a) diameter and (b) G/D ratio.

These experimental data demonstrate that the larger average diameter SWCNT forests are conducive for higher electrical conductivity and that the influence of the defect level on the electrical conductance is much less significant than on the thermal diffusivity.

Generally, the synthesized SWCNT forests consist of a mixture of semiconducting and metallic SWCNTs. One of the unique aspects of SWCNTs is that the semiconducting band gap is inversely related to the diameter.[4] This means that larger diameter CNTs generally possess more metallic behavior and thus should be more conductive, whereas smaller diameter CNTs are generally more semiconducting. Theoretical calculation predicts that a 1.5 nm semiconducting SWCNT possesses a 0.53 eV band gap and a 3 nm SWCNT possesses a 0.27 eV band gap. In addition, experiments have shown that metallic CNTs exhibit an electrical conductivity 1 order higher than semiconducting CNTs.[1,37,38] We interpret that the observed increase in electrical sheet conductance of SWCNT forests is a result of the reduced average band gap. Interestingly as the electrical sheet conductance did not significantly depend on the defect level, the defect level was not the rate-limiting process for electron transport in SWCNT forests. Theoretical calculations also show that electron transport is much more tolerant to crystalline defects than phonon transport.[32,33,39,40] As a result, SWCNT forests with large average diameter exhibited high electrical conductances despite possessing low G/D ratios (high defect levels).

For the SWCNT forests with different diameters and defect levels, the thermal properties were plotted *versus* electrical properties in two identical Ashby maps, one color-coded by diameter and the other by G/D ratio (Figure 4). The map shows the inverse relationship between thermal diffusivity and electrical sheet conductance, and particularly, the region of high thermal diffusivity and high electrical sheet conductance was curiously vacant. On the basis of previous discussions, this mutual exclusivity results from a combination of three phenomena. First, the processes governing phonon transport (*e.g.*, Umklapp scattering) and electron transport (*e.g.*, band gap) exhibit opposite trends with diameter. Second, small diameter SWCNTs could be synthesized with low defect levels (high crystallinity), which was crucial for high thermal diffusivity. Third, electron transport is more tolerant to defects than phonon transport enabling the band gap to be the dominant process for electrical properties at large diameter SWCNT forests, which could only

be synthesized with high defect levels. These interpretations on the mutual exclusivity between thermal diffusivity and electrical conductance of SWCNT forests would generally apply to CNT synthesis systems. The implication of this result is that the "ideal" SWCNT forest structure would likely differ from application to application.

Our results strongly suggest that within conventional CVD synthesis techniques, synthesis of an "ideal" SWCNT forest structure that simultaneously possesses the highest thermal and electrical conductivities is extremely difficult. In principle, a small diameter, highly crystalline, and all metallic SWCNT forest is expected to possess both high electrical and thermal properties, but as far as synthesis technology has recently advanced, it has not yet reached that level of control. In fact, many studies on controlled and selective synthesis of CNTs have shown that the reported control cannot be achieved without sacrifice to another structural property, commonly yield.[5,41−45] These results indicate that even if an "ideal" SWCNT could be synthesized, advancement to commercial applications would be difficult.

CONCLUSION

To conclude, this investigation between the structure and property for SWCNTs within a vertically aligned forest represents a new research and an important direction to extract their fundamental relationship. In so doing, we have gained understanding of the intrinsic electrical and thermal properties of SWCNTs on their structures to provide a more general and fundamental knowledge of the most suitable CNT for a particular application. This study was made possible through recent advancements in the CNT synthetic technology, which allowed for the continuous structural control over a wide range. Through these means, graphs of the property as a function of the structure and a different property could be constructed to understand not only their relationship, but, equally important, their limitations, both technically and fundamentally. In this work, we found an inverse relationship between the thermal diffusivity and the electrical conductance which showed a fundamental mutual exclusivity between the two properties. This relationship was further explained by the differences in the fundamental mechanisms governing each property and the optimum required structures. Further, we learned that within typical CVD synthesis techniques, it is extremely difficult to synthesize an "ideal" SWCNT forest structure that simultaneously possesses the highest thermal and electrical conductivities. We hope that this work would act as an impetus for future work in examining other structural relationships on SWCNT and CNT properties.

EXPERIMENTAL METHODS

Synthesis. Aluminum film with a thickness of 5 nm was sputtered on Si substrate, followed by an oxygen plasma treatment. Then, Fe film (0.5−2.5 nm) and Al film (0.5−2.0 nm) were separately sputtered to form the trilayer structure. The formation phase was carried out at different formation temperature (550−750 °C) in 90% H_2 with He as carrier gas, followed by a growth phase at 750 °C with 1% C_2H_4 in He.

Characterization. G/D ratio of SWCNT forests was characterized by Raman spectroscopy (Thermo-Electron Raman Spectrometer) with an excitation wavelength of 532 nm. The average diameter of SWCNT forests was evaluated by Fourier transform infrared spectroscopy (FT-IR, Nicolet 6700) by converting the position of S_{11} absorbance peak and confirmed by transmission electron microscopy (Hitachi H-9000NA). The thermal diffusivity of SWCNT forests was measured in air under ambient temperature by the flash method using a Xenon lamp (NETZSCH, LFA 447 NanoFlash). The electrical sheet conductance of SWCNT forests was the inverse of the sheet resistance measured by a lithographically fabricated micro-4-probe.

Conflict of Interest: The authors declare no competing financial interest.

Acknowledgment. Support by Technology Research Association for Single Wall Carbon Nanotubes (TASC) is acknowledged. The authors wish to acknowledge J. He and L. Yu for their technical assistance.

Supporting Information Available: CNT diameter as a function of catalyst Fe film thickness, and CNT number density in SWCNT forests *versus* diameter. This material is available free of charge *via* the Internet at http://pubs.acs.org.

REFERENCES AND NOTES

1. Ebbesen, T. W.; Lezec, H. J.; Hiura, H.; Bennett, J. W.; Ghaemi, H. F.; Thio, T. Electrical Conductivity of Individual Carbon Nanotubes. *Nature* **1996**, *382*, 54–56.
2. Fujii, M.; Zhang, X.; Xie, H. Q.; Ago, H.; Takahashi, K.; Ikuta, T.; Abe, H.; Shimizu, T. Measuring the Thermal Conductivity of a Single Carbon Nanotube. *Phys. Rev. Lett.* **2005**, *95*, 065502−1–065502−4.
3. Li, Q. W.; Li, Y.; Zhang, X. F.; Chikkannanavar, S. B.; Zhao, Y. H.; Dangelewicz, A. M.; Zheng, L. X.; Doorn, S. K.; Jia, Q. X.; Peterson, D. E.; *et al.* Structure-Dependent Electrical Properties of Carbon Nanotube Fibers. *Adv. Mater.* **2007**, *19*, 3358–3363.
4. Wildöer, J. W. G.; Venema, L. C.; Rinzler, A. G.; Smalley, R. E.; Dekker, C. Electronic Structure of Atomically Resolved Carbon Nanotubes. *Nature* **1998**, *391*, 59–62.
5. Ding, L.; Tselev, A.; Wang, J. Y.; Yuan, D. N.; Chu, H. B.; McNicholas, T. P.; Li, Y.; Liu, J. Selective Growth of Well-Aligned Semiconducting Single-Walled Carbon Nanotubes. *Nano Lett.* **2009**, *9*, 800–805.
6. Esconjauregui, S.; Fouquet, M.; Bayer, B. C.; Ducati, C.; Smajda, R.; Hofmann, S.; Robertson, J. Growth of Ultrahigh Density Vertically Aligned Carbon Nanotube Forests for Interconnects. *ACS Nano* **2010**, *4*, 7431–7436.
7. Liu, Q. F.; Ren, W. C.; Chen, Z. G.; Wang, D. W.; Liu, B. L.; Yu, B.; Li, F.; Cong, H. T.; Cheng, H. M. Diameter-Selective Growth of Single-Walled Carbon Nanotubes with High Quality by Floating Catalyst Method. *ACS Nano* **2008**, *2*, 1722–1728.
8. Chiang, W. H.; Sankaran, R. M. Linking Catalyst Composition to Chirality Distributions of as-Grown Single-Walled Carbon Nanotubes by Tuning Ni_xFe_{1-x} Nanoparticles. *Nat. Mater.* **2009**, *8*, 882–886.

9. Jackson, J. J.; Puretzky, A. A.; More, K. L.; Rouleau, C. M.; Eres, G.; Geohegan, D. B. Pulsed Growth of Vertically Aligned Nanotube Arrays with Variable Density. *ACS Nano* **2010**, *4*, 7573–7581.
10. Xiang, R.; Einarsson, E.; Murakami, Y.; Shiomi, J.; Chiashi, S.; Tang, Z. K.; Maruyama, S. Diameter Modulation of Vertically Aligned Single-Walled Carbon Nanotubes. *ACS Nano* **2012**, *6*, 7472–7479.
11. Zhao, B.; Futaba, D. N.; Yasuda, S.; Akoshima, M.; Yamada, T.; Hata, K. Exploring Advantages of Diverse Carbon Nanotube Forests with Tailored Structures Synthesized by Supergrowth from Engineered Catalysts. *ACS Nano* **2009**, *3*, 108–114.
12. Xu, M.; Futaba, D. N.; Yumura, M.; Hata, K. Alignment Control of Carbon Nanotube Forest from Random to Nearly Perfectly Aligned by Utilizing the Crowding Effect. *ACS Nano* **2012**, *6*, 5837–5844.
13. Sakurai, S.; Inaguma, M.; Futaba, D. N.; Yumura, M.; Hata, K. Diameter and Density Control of Single-Wall Carbon Nanotube Forests by Modulating Ostwald Ripening through Decoupling the Catalyst Formation and Growth Processes. *Small* **2013**, 10.1002/smll.201300223.
14. Sakurai, S.; Nishino, H.; Futaba, D. N.; Yasuda, S.; Yamada, T.; Maigne, A.; Matsuo, Y.; Nakamura, E.; Yumura, M.; Hata, K. Role of Subsurface Diffusion and Ostwald Ripening in Catalyst Formation for Single-Walled Carbon Nanotube Forest Growth. *J. Am. Chem. Soc.* **2012**, *134*, 2148–2153.
15. Chen, G. H.; Neupane, S.; Li, W. Z.; Chen, L. N.; Zhang, J. D. An Increase in the Field Emission from Vertically Aligned Multiwalled Carbon Nanotubes Caused by NH_3 Plasma Treatment. *Carbon* **2013**, *52*, 468–475.
16. Dai, H. J.; Wong, E. W.; Lieber, C. M. Probing Electrical Transport in Nanomaterials: Conductivity of Individual Carbon Nanotubes. *Science* **1996**, *272*, 523–526.
17. Berber, S.; Kwon, Y. K.; Tomanek, D. Unusually High Thermal Conductivity of Carbon Nanotubes. *Phys. Rev. Lett.* **2000**, *84*, 4613–4616.
18. Zhang, D. H.; Ryu, K.; Liu, X. L.; Polikarpov, E.; Ly, J.; Tompson, M. E.; Zhou, C. W. Transparent, Conductive, and Flexible Carbon Nanotube Films and Their Application in Organic Light-Emitting Diodes. *Nano Lett.* **2006**, *6*, 1880–1886.
19. Tchoul, M. N.; Ford, W. T.; Ha, M. L. P.; Chavez-Sumarriva, I.; Grady, B. P.; Lolli, G. L.; Resasco, D. E.; Arepalli, S. Composites of Single-Walled Carbon Nanotubes and Polystyrene: Preparation and Electrical Conductivity. *Chem. Mater.* **2008**, *20*, 3120–3126.
20. Ata, S.; Kobashi, K.; Yumura, M.; Hata, K. Mechanically Durable and Highly Conductive Elastomeric Composites from Long Single-Walled Carbon Nanotubes Mimicking the Chain Structure of Polymers. *Nano Lett.* **2012**, *12*, 2710–2716.
21. De, S.; Lyons, P. E.; Sorel, S.; Doherty, E. M.; King, P. J.; Blau, W. J.; Nirmalraj, P. N.; Boland, J. J.; Scardaci, V.; Joimel, J.; *et al.* Transparent, Flexible, and Highly Conductive Thin Films Based on Polymer−Nanotube Composites. *ACS Nano* **2009**, *3*, 714–720.
22. Hata, K.; Futaba, D. N.; Mizuno, K.; Namai, T.; Yumura, M.; Iijima, S. Water-Assisted Highly Efficient Synthesis of Impurity-Free Single-Walled Carbon Nanotubes. *Science* **2004**, *306*, 1362–1364.
23. Zhong, G. F.; Iwasaki, T.; Honda, K.; Furukawa, Y.; Ohdomari, I.; Kawarada, H. Low Temperature Synthesis of Extremely Dense, and Vertically Aligned Single-Walled Carbon Nanotubes. *Jpn. J. Appl. Phys.* **2005**, *44*, 1558–1561.
24. Zhong, G. F.; Warner, J. H.; Fouquet, M.; Robertson, A. W.; Chen, B. A.; Robertson, J. Growth of Ultrahigh Density Single-Walled Carbon Nanotube Forests by Improved Catalyst Design. *ACS Nano* **2012**, *6*, 2893–2903.
25. Wirth, C. T.; Bayer, B. C.; Gamalski, A. D.; Esconjauregui, S.; Weatherup, R. S.; Ducati, C.; Baehtz, C.; Robertson, J.; Hofmann, S. The Phase of Iron Catalyst Nanoparticles During Carbon Nanotube Growth. *Chem. Mater.* **2012**, *24*, 4633–4640.
26. Parker, W. J.; Jenkins, R. J.; Abbott, G. L.; Butler, C. P. Flash Method of Determining Thermal Diffusivity, Heat Capacity, and Thermal Conductivity. *J. Appl. Phys.* **1961**, *32*, 1679–1684.
27. Kim, P.; Shi, L.; Majumdar, A.; McEuen, P. L. Thermal Transport Measurements of Individual Multiwalled Nanotubes. *Phys. Rev. Lett.* **2001**, *87*, 215502–1−215502−4.
28. Pop, E.; Mann, D.; Wang, Q.; Goodson, K. E.; Dai, H. J. Thermal Conductance of an Individual Single-Wall Carbon Nanotube above Room Temperature. *Nano Lett.* **2006**, *6*, 96–100.
29. Cao, J. X.; Yan, X. H.; Xiao, Y.; Ding, J. W. Thermal Conductivity of Zigzag Single-Walled Carbon Nanotubes: Role of the Umklapp Process. *Phys. Rev. B* **2004**, *69*, 073407−1–073407−4.
30. Hone, J.; Whitney, M.; Piskoti, C.; Zettl, A. Thermal Conductivity of Single-Walled Carbon Nanotubes. *Phys. Rev. B* **1999**, *59*, R2514–R2516.
31. Yu, C. H.; Shi, L.; Yao, Z.; Li, D. Y.; Majumdar, A. Thermal Conductance and Thermopower of an Individual Single-Wall Carbon Nanotube. *Nano Lett.* **2005**, *5*, 1842–1846.
32. Che, J. W.; Cagin, T.; Goddard, W. A. Thermal Conductivity of Carbon Nanotubes. *Nanotechnology* **2000**, *11*, 65–69.
33. Sevik, C.; Sevincli, H.; Cuniberti, G.; Cagin, T. Phonon Engineering in Carbon Nanotubes by Controlling Defect Concentration. *Nano Lett.* **2011**, *11*, 4971–4977.
34. Shamsa, M.; Liu, W. L.; Balandin, A. A.; Casiraghi, C.; Milne, W. I.; Ferrari, A. C. Thermal Conductivity of Diamond-Like Carbon Films. *Appl. Phys. Lett.* **2006**, *89*, 161921–1−161921−3.
35. Haskins, J.; Kinaci, A.; Sevik, C.; Sevincli, H.; Cuniberti, G.; Cagin, T. Control of Thermal and Electronic Transport in Defect-Engineered Graphene Nanoribbons. *ACS Nano* **2011**, *5*, 3779–3787.
36. Ivanov, I.; Puretzky, A.; Eres, G.; Wang, H.; Pan, Z. W.; Cui, H. T.; Jin, R. Y.; Howe, J.; Geohegan, D. B. Fast and Highly Anisotropic Thermal Transport through Vertically Aligned Carbon Nanotube Arrays. *Appl. Phys. Lett.* **2006**, *89*, 223110−1–223110−3.
37. Chattopadhyay, D.; Galeska, L.; Papadimitrakopoulos, F. A Route for Bulk Separation of Semiconducting from Metallic Single-Wall Carbon Nanotubes. *J. Am. Chem. Soc.* **2003**, *125*, 3370–3375.
38. Skakalova, V.; Kaiser, A. B.; Woo, Y. S.; Roth, S. Electronic Transport in Carbon Nanotubes: From Individual Nanotubes to Thin and Thick Networks. *Phys. Rev. B* **2006**, *74*, 085403–1−085403−10.
39. Chico, L.; Benedict, L. X.; Louie, S. G.; Cohen, M. L. Quantum Conductance of Carbon Nanotubes with Defects. *Phys. Rev. B* **1996**, *54*, 2600–2606.
40. Grujicic, M.; Cao, G.; Singh, R. The Effect of Topological Defects and Oxygen Adsorption on the Electronic Transport Properties of Single-Walled Carbon-Nanotubes. *Appl. Surf. Sci.* **2003**, *211*, 166–183.
41. Kimura, H.; Futaba, D. N.; Yumura, M.; Hata, K. Mutual Exclusivity in the Synthesis of High Crystallinity and High Yield Single-Walled Carbon Nanotubes. *J. Am. Chem. Soc.* **2012**, *134*, 9219–9224.
42. Sakurai, S.; Inaguma, M.; Futaba, D. N.; Yumura, M.; Hata, K. A Fundamental Limitation of Small Diameter Single-Walled Carbon Nanotube Synthesis-a Scaling Rule of the Carbon Nanotube Yield with Catalyst Volume. *Materials* **2013**, *6*, 2633–2641.
43. Qu, L. T.; Du, F.; Dai, L. M. Preferential Syntheses of Semiconducting Vertically Aligned Single-Walled Carbon Nanotubes for Direct Use in FETs. *Nano Lett.* **2008**, *8*, 2682–2687.
44. Harutyunyan, A. R.; Chen, G. G.; Paronyan, T. M.; Pigos, E. M.; Kuznetsov, O. A.; Hewaparakrama, K.; Kim, S. M.; Zakharov, D.; Stach, E. A.; Sumanasekera, G. U. Preferential Growth of Single-Walled Carbon Nanotubes with Metallic Conductivity. *Science* **2009**, *326*, 116–120.
45. Hong, G.; Zhang, B.; Peng, B. H.; Zhang, J.; Choi, W. M.; Choi, J. Y.; Kim, J. M.; Liu, Z. F. Direct Growth of Semiconducting Single-Walled Carbon Nanotube Array. *J. Am. Chem. Soc.* **2009**, *131*, 14642–14643.